A 3D-NMR Method for Studying Hydrocarbon-Based Polymer Structures

Masud Monwar, Sangrama K. Sahoo, and Peter L. Rinaldi*

Department of Chemistry, University of Akron, Akron, Ohio 44325-3601

Elizabeth F. McCord and Donald R. Marshall

Dupont Experimental Station, Bldg 328, Rm 133, Route 141 and Powder Mill Rd., Wilmington, Delaware 19880-328

Michael Buback and Henning Latz

Institut für Physikalische Chemie, Universität Göttingen, Tammannstr. 6, D 37077 Göttingen, Germany

Received May 27, 2003

High-field NMR chemical shifts are sensitive to minor changes in the polymer structure and are of great help in characterizing the structures and compositions of polymers. This information is vital to determine structure−property relationships used in synthesizing new polymers and in modifying the properties of existing polymers. Thorough characterizations of copolymers using high-field 1D- and 2D-NMR are now routine procedures. However, almost no work has been done on terpolymers, especially ethylene-containing terpolymers, due to the numerous structures present from branching and monomer- and stereo-sequence effects. These factors lead to enormously complex NMR spectra which pose quite a challenge for unambiguous interpretation of spectral information.

Triple-resonance $^{1}H/^{13}C/X$ 3D-NMR techniques have been used to simplify the spectra of the complex polymers by dispersing the $^{1}H-^{13}C$ correlated 2D NMR resonances into a third (X-nucleus chemical shift) dimension.[1] These techniques have been applied to study the structures and stereosequence distributions of a variety of fluoropolymers,[2] to identify resonances from the chain ends formed by diphenylphosphinyl radical initiated styrene polymerization[3] and tri-*n*-butyltin-capped polybutadiene,[4] and to characterize the structures and tacticities of polysilanes[5] and polycarbosilanes.[6] All of these applications are based on the presence of a heteroatom (X) such as ^{31}P, ^{19}F, ^{29}Si, or ^{119}Sn in the polymer. Unfortunately, most of the synthetic polymers of research and commercial significance are hydrocarbon-based and lack a third NMR-active nucleus.

Here, a new multidimensional NMR methodology for characterizing hydrocarbon-based polymers is described. This methodology involves the use of selective ^{13}C-labeling of the polymer and selective excitation[7,8] of the resonances from the labeled site as if they were from a third NMR-active X-nucleus, to produce greatly simplified 3D-NMR spectra. The methodology is illustrated using a sample of poly(ethylene-*co*-*n*-butyl acrylate-*co*-carbon monoxide) (polyEBC) prepared from 1-^{13}C-*n*-butyl acrylate ($CH_2{=}CH-{}^{13}CO_2-n\text{-}C_4H_9$). The 1D ^{13}C and 2D $^{1}H-^{13}C$ NMR spectra of this terpolymer are complex because of the large number of possible *n*-ads produced by both monomer- and stereo-sequence effects as well as the presence of branching structures produced by backbiting reactions.[9] Triple-resonance 3D-NMR combined with selective ^{13}C-labeling is a solution to this problem as it greatly simplifies the atomic connectivity information among three different nuclei. Incorporation of ^{13}C-labeled *n*-butyl acrylate (B) monomers results in selective enhancement of B-centered *n*-ad resonances, producing further spectral simplification.

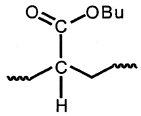

1

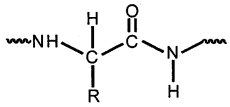

2

Identification of the H−C−CO structure fragment of a B-centered triad (**1**) in polyEBC can be viewed in parallel to a similar problem of identifying the H−C−CO structure fragment of a peptide unit **2** in a protein backbone. The NMR solution to this problem in polyEBC can be attained using the HCACO pulse sequence,[10] used to determine the $^{1}H-^{13}C_{\alpha}-^{13}C{=}O$ connectivity in protein NMR studies. This sequence performs coherence transfer through the $^{1}H-^{13}C_{\alpha}-^{13}C{=}O$ bonding framework to produce a correlation in a 3D-NMR spectrum that yields atomic connectivity information among these three atoms within a monomer unit of a polypeptide. The major difference is that proteins studied by multidimensional NMR methods are uniformly labeled with ^{15}N and ^{13}C, whereas in this case, the terpolymer is selectively labeled in only one position. Consequently, there is an additional challenge of suppressing the $^{1}H-^{12}C-^{13}C{=}O$ resonances from 99% of the structure fragments, while selectively detecting 1% of the B-centered triads containing the $^{1}H-^{13}C-^{13}C{=}O$ isotope fragments. While protein NMR is generally performed in H_2O, polymer spectroscopy is generally performed in perdeuterated organic solvents. To a large degree, this reduces the strength of solvent proton resonances which must be suppressed in polymer spectroscopy. However, it is not possible to use $^{1}H-^{13}C$ coherence selection and pulsed field gradient/diffusion methods such as WATERGATE[11] as aids in solvent suppression as is routinely done in protein NMR.

The 1D ^{13}C NMR spectrum of the labeled polyEBC (see Supporting Information) shows the expected enhancement of the ester−carbonyl resonances (∼175 ppm), from selective ^{13}C-labeling of B fragments, when compared with a spectrum of a similar, unlabeled polyEBC sample. Some of the resonances in the aliphatic region of the labeled polymer are broadened or split due to the presence of $^{13}C-^{13}C$ homonuclear *J*-coupling to the carbonyl carbons. This splitting is not observed in the spectrum of unlabeled polymer due to the low occurrence of doubly labeled $^{13}C-^{13}C$ fragments. Other differences between these spectra arise because the unlabeled sample is a commercial polymer produced in a continuous flow reactor, while the labeled polymer is made in the laboratory with a minipilot, batch reactor. Although the relative intensities of the signals in the two spectra are different, the same sets of resonances are observed in the spectra of both polymer samples. The ester−carbonyl region is extremely complex, containing over two dozen overlapping resonances.

Figure 1 shows a pulse sequence used to collect gradient HCACO (*g*HCACO) 3D-NMR data. Although,

* Corresponding author: Tel 330-972-5990; Fax 330-972-5256; e-mail PeterRinaldi@uakron.edu.

10.1021/ma030292z CCC: $25.00
Published on Web 08/14/2003

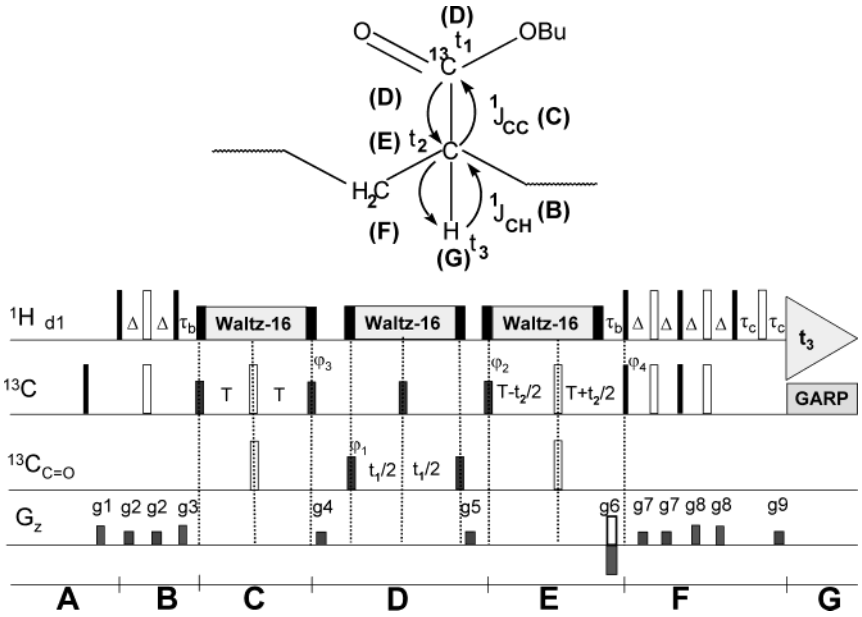

Figure 1. Three-dimensional *g*HCACO NMR pulse sequence used for the $^1H-^{13}C_\alpha-^{13}C{=}O$ correlation experiment. Unless otherwise stated, the solid and open bars represent $\pi/2$ and π pulses, respectively. All pulses were applied along the *x*-axis if not indicated otherwise. The $^{13}C{=}O$ and $^{13}C_\alpha$ transmitters were centered at 174.0 and 42.0 ppm, respectively. The delays employed were $\Delta = 1.9$ ms, $\tau_b = 3.3$ ms, $\tau_c = 0.2$ ms, and $2T = 21.7$ ms. The phase cycling employed were $\varphi_1 = 2(x), 2(-x)$; $\varphi_2 = x, -x$; $\varphi_3 = 4(y), 4(-y)$; $\varphi_4 = x$. The $^1H-^{13}C$ coherence selection is achieved by the gradient pair g6 and g9 in a 4:1 ratio. The strengths and durations of the gradients are $g0 = 0.08$ T/m, 0.5 ms; $g1 = 0.28$ T/m, 0.5 ms; $g2 = 0.15$ T/m, 0.5 ms; $g3 = 0.30$ T/m, 1.0 ms; $g4 = 0.20$ T/m, 0.3 ms; $g5 = 0.15$ T/m, 0.2 ms; $g6 = 0.15$ T/m, 1.6 ms; $g7 = 0.15$ T/m, 0.6 ms; $g8 = 0.25$ T/m, 0.4 ms and $g9 = 0.15$ T/m, 0.4 ms. Quadrature detection in t_1 is achieved using the States-TPPI[17] method by incrementing the phase of the ϕ_1. Echo/antiecho selection during t_2 was achieved by inverting the phase of ϕ_4 and inverting the sign of the *g*6 gradient.

for purposes of clarity, this figure shows a three-channel version of the sequence, the data presented in the figures below were obtained with a two-channel version of the pulse sequence (see Supporting Information for details). This is accomplished by shifting the ^{13}C decoupler offset between the $^{13}C_\alpha$ to $^{13}C{=}O$ region and use of a shifted laminar pulse[8] for selective inversion of $^{13}C_\alpha$ resonances during the $^{13}C{=}O$ chemical shift evolution period. This sequence is a variation of the standard HCACO[10] experiment used in biomolecular NMR structure determination. It has been modified to eliminate the water suppression features of the experiment, and the delays based on the default *J*-couplings found in proteins have been replaced with values appropriate for the polymer structures of interest here. In addition, the standard offsets and spectral windows that are used for the amide carbonyl and α-CH resonances of proteins have been replaced by user enterable values (offsets and phase shifting in shifted laminar pulses are determined based on these offsets) that are appropriate for these polymers.

This pulse sequence works by sequential INEPT[12] magnetization transfer steps from ^1H to the $^{13}C_{aliphatic}$ atoms (α to the carbonyl, period B) using $^1J_{CH}$; then from $^{13}C_{aliphatic}$ to $^{13}C_{C=O}$ (period C) using $^1J_{CC}$; the t_1 evolution period is used to encode the carbonyl carbon shifts (period D) and to accomplish reverse INEPT transfer of magnetization from $^{13}C_{C=O}$ to $^{13}C_{aliphatic}$; a constant evolution time $2T$ is used to encode the $^{13}C_{aliphatic}$ chemical shifts in the t_2 evolution time (period E); a reverse INEPT transfer from $^{13}C_{aliphatic}$ to ^1H is performed (period F); and antiphase magnetization created during the beginning of the sequence is refocused during the second pair of delays (period F) before detection of the protons during the acquisition time t_3. During the magnetization transfer from $^{13}C_\alpha$ to $^{13}C{=}O$ and during t_1 and t_2 evolution, the transverse magnetization of $^1H_\alpha$ is locked along the *x*-axis by a Waltz-16[13] spin-lock, so that homonuclear couplings between $^1H_\alpha$ and other protons are removed. The spin-lock field was kept low in order to avoid homonuclear Hartmann−Hahn effects.[14]

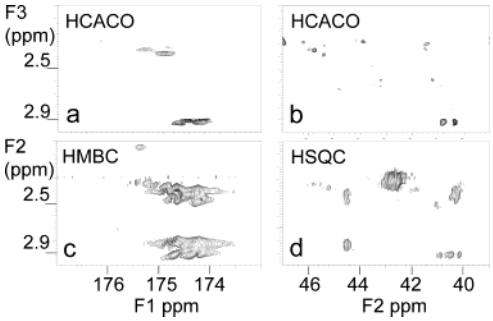

Figure 2. 2D-NMR spectra of polyEBC labeled at the ester carbonyl of B: (a) *f*1*f*3 plane from the truncated 3D *g*HCACO NMR spectrum showing the two-bond $^1H-^{13}C_\alpha-^{13}C{=}O$ correlations; (b) *f*2*f*3 plane from truncated 3D *g*HCACO NMR spectrum showing the one-bond $^1H-^{13}C_\alpha-^{13}C{=}O$ correlations; (c) $^1H-^{13}C$ *g*HSQC NMR spectrum of the aliphatic (39.0−47.0 ppm) region; and (d) $^1H-^{13}C$ *g*HMBC NMR spectrum showing correlations between ester−carbonyl carbons and methine protons (173.0−177.0 ppm).

As a prelude to $^1H-^{13}C$ chemical shift correlated 2D-NMR spectral data acquisition (such as HSQC[15] and HMBC[16]), 1D ^1H and ^{13}C spectra are obtained when sensitivity permits. Similarly, as a prelude to collection of 3D-NMR spectra, two "truncated" 3D-NMR spectra are collected by fixing t_2 and t_1 to produce the first 2D planes in the *f* 1*f* 3 (Figure 2a) and *f* 2*f* 3 (Figure 2b) dimensions of the 3D-NMR spectra, respectively. These planes exhibit two-bond $^1H-^{13}C_\alpha-^{13}C{=}O$ (Figure 2a) and one-bond $^1H-^{13}C_\alpha-^{13}C{=}O$ (Figure 2b) correlations much like those observed in the *g*HMBC (Figure 2c) and *g*HSQC (Figure 2d) 2D-NMR spectra. However, the standard 2D-NMR spectra show all the possible

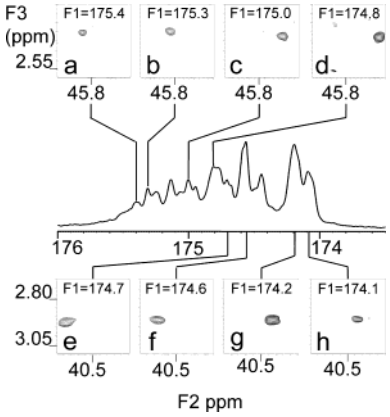

Figure 3. Slices from the 3D *g*HCACO NMR spectrum showing the one-bond $^1H-^{13}C_\alpha-^{13}C{=}O$ correlations at different $^{13}C{=}O$ chemical shifts in polyEBC. An expansion of the ^{13}C-labeled ester carbonyl region from the 1D ^{13}C spectrum is shown in the center, with lines relating the slices corresponding to the carbonyl peaks. The total experiment time was ca. 28 h. The data were linear predicted to 4 times the original number of increments in both t_1 and t_2 dimensions and were zero-filled to 512 × 512 × 4096 complex points and weighted with a sinebell and shifted sinebell function before Fourier transformation.

C−H correlations, while all the resonances except those from structure fragments bound to the labeled ester−carbonyl are filtered from the truncated 3D-NMR spectra. The cross-peaks in the truncated 3D spectra in Figure 2a,b are also considerably simpler than the corresponding cross-peaks in the *g*HMBC and *g*HSQC 2D-NMR spectra in Figure 3c,d. This is because the constant evolution period E and the selective $^{13}C_\alpha$ inversion pulse in the middle of period D remove ^{13}C homonuclear couplings in the indirectly detected $f1$ and $f2$ dimensions of the 3D-NMR spectra, while these couplings are evident in the indirectly detected ($f1$) dimensions of the HMBC and HSQC 2D-NMR spectra.

Figure 3 shows slices from the methine region of the 3D-NMR spectrum at selected C=O chemical shifts in the $f1$ dimension. The $f1$ shifts are labeled at the top of each slice, and the individual planes are correlated with their respective carbonyl resonances in the expansion of the ester carbonyl region from the 1D ^{13}C NMR spectrum shown in the center of Figure 3. The full 3D-NMR spectrum permits clear resolution of 36 separate sets of resonances in unique, resolvable $f1$ planes. The cross-peaks observed at $\delta_H \sim 2.32$ ppm with carbon resonances $\delta_C \sim 45$ ppm and those at $\delta_H \sim 2.92$ ppm with $\delta_C \sim 40$ ppm in the 2D HSQC spectrum are also observed here. However, in Figure 3 there is additional information proving connectivity with the ester−carbonyl carbons. Thus, the overlapped peaks in the *g*HMBC spectrum can be dispersed and resolved with this 3D-NMR experiment, and information contributing to the complete and unequivocal resonance assignments of the B-centered triads is obtained.

While it is usually difficult and prohibitively expensive to obtain uniformly labeled synthetic polymers at this time, it is usually possible to perform selective labeling of interesting parts of synthetic polymers. Once these labeled polymers are obtained, a modified gradient *g*HCACO pulse sequence[10] is quite useful for collection of 3D-NMR spectra from hydrocarbon-based polymers such as polyEBC. The spectra of the terpolymers are very complex, and 3D-NMR methods provide enormous spectral simplification, peak resolution, and chemical shift dispersion. The unique chemical shift correlations provide detailed structural information. This and related methods of simplifying the NMR spectra will be generally useful for studying the complex mixtures of structures like those found in terpolymers; the 3D-NMR methodology can easily be extended to solve many other problems in organic structure determination. More importantly, this work shows that variations of the many 3D-NMR experiments used to study protein structure should be adaptable to the study of synthetic polymer structures. When the results from several of these methods are used together, detailed structures should be identifiable, even in the most complex polymers.

Acknowledgment. The authors acknowledge the National Science Foundation (DMR-0073346) and E.I. du Pont de Nemours and Co for support of this research and the Kresge Foundation and donors to the Kresge Challenge program at the University of Akron for funds used to purchase the 750 MHz NMR instrument used for this work. Thanks are due to V. Dudipala, J. Massey, and S. Stakleff for their support in maintaining the NMR facilities used in this work.

Supporting Information Available: One-dimensional ^{13}C NMR spectra and experimental details for preparation of the labeled polymer and collection of 3D-NMR data. This material is available free of charge via the Internet at http://pubs.acs.org.

References and Notes

(1) Rinaldi, P. L. In *NMR Spectroscopy of Polymers in Solution and in the Solid State*; Cheng, H. N., English, A. D., Eds.; ACS Symposium Series 834; American Chemical Society: Washington, DC, 2003; Chapter 8, p 94.
(2) (a) Rinaldi, P. L.; Ray, D. G., III; Li, L.; Wang, H. T.; Harwood, H. J. *Multidimensional Spectroscopy of Polymers*; Urban, M. W., Provder, T., Eds.; ACS Symposium Series 598; American Chemical Society: Washington, DC, 1995; Chapter 13. (b) Li, L.; Ray, D. G., III; Wang, H. T.; Harwood, H. J.; Rinaldi, P. L. *Macromolecules* **1996**, *29*, 4706. (c) Rinaldi, P. L.; Ray, D. G., III; Li, L.; Wang, H. T.; Harwood, H. J. *Polym. Mater. Sci. Eng.* **1994**, *71*, 269. (d) Li, L.; Rinaldi, P. L. *Macromolecules* **1996**, *29*, 4808. (e) Li, L.; Rinaldi, P. L. *Macromolecules* **1997**, *30*, 520.
(3) (a) Saito, T.; Medsker, R. E.; Harwood, H. J.; Rinaldi, P. L. *J. Magn. Reson., Ser. A* **1996**, *120*, 125. (b) Meng, H.; Saito, T.; Rinaldi, P. L.; Wyzgoski, F.; Helfer, C. A.; Mattice, W. L.; Harwood, H. J. *Macromolecules* **2001**, *34*, 801.
(4) Liu, W.; Saito, T.; Li, L.; Rinaldi, P. L.; Hirst, R.; Halasa, A. F.; Visintainer, J. *Macromolecules* **2000**, *33*, 2364.
(5) Liu, W.; Rinaldi, P. L.; Galya, L.; Hansen, J. E.; Wilczek, L. *Organometallics* **2002**, *21*, 3250.
(6) Chai, M.; Tessier, C.; Rinaldi, P. L. *J. Am. Chem. Soc.* **1999**, *121*, 273.
(7) Freeman, R. *Prog. Nucl. Magn. Reson. Spectrosc.* **1998**, *32*, 59.
(8) Patt, S. L. *J. Magn. Reson.* **1992**, *96*, 94.
(9) McCord, E. F.; Shaw, W. H., Jr.; Hutchinson, R. A. *Macromolecules* **1997**, *30*, 246.
(10) (a) Kay, L. E.; Ikura, M.; Tschudin, R.; Bax, A. *J. Magn. Reson.* **1990**, *89*, 496. (b) Kay, L. E.; Ikura, M.; Bax, A. *J. Magn. Reson.* **1991**, *91*, 84.
(11) Sklenar, V.; Piotto, M.; Leppik, R.; Saudec, V. *J. Magn. Reson., Ser. A* **1993**, *102*, 241.
(12) Morris, G. A.; Freeman, R. *J. Am. Chem. Soc.* **1979**, *101*, 760.
(13) Shaka, A. J.; Keeler, J.; Freeman, R. *J. Magn. Reson.* **1983**, *52*, 335.
(14) Xia, Y.; Kong, X.; Smith, D. K.; Liu, Y.; Man, D.; Zhu, G. *J. Magn. Reson.* **2000**, *143*, 407.
(15) Bodenhausen, G.; Ruben, D. J. *Chem. Phys. Lett.* **1980**, *69*, 565.
(16) Bax, A.; Summers, M. F. *J. Am. Chem.* Soc. **1986**, *108*, 2093.
(17) Marion, D.; Ikura, M.; Tschudin, R.; Bax, A. *J. Magn. Reson.* **1989**, *85*, 393.

MA030292Z